Diagnostic and Interventional Imaging (2019) **100**, 17—23

ORIGINAL ARTICLE /*Research and new developments*

# In-vitro validation of 4D flow MRI measurements with an experimental pulsatile flow model

**A. David**[a,*], **D. Le Touze**[b], **K. Warin-Fresse**[a], **P. Paul-Gilloteaux**[c], **F. Bonnefoy**[b], **J. Idier**[d], **S. Moussaoui**[d], **P. Guerin**[e], **J.-M. Serfaty**[a,f]

[a] *Department of cardiovascular imaging, centre hospitalier universitaire de Nantes, 44800 Saint-Herblain, France*
[b] *Laboratoire de recherche en hydrodynamique, énergétique et environnement (CNRS, UMR 6598), École centrale Nantes, 44321 Nantes cedex 3, France*
[c] *Structure fédérative de recherche santé François-Bonamy, institut de recherche en santé de l'université de Nantes, 44007 Nantes cedex 1, France*
[d] *Laboratoire des sciences du numérique de Nantes (LS2N, UMR CNRS 6004), École centrale de Nantes, 44321 Nantes cedex 3, France*
[e] *Department of cardiology, centre hospitalier universitaire de Nantes, 44800 Saint-Herblain, France*
[f] *Unité de recherche Inserm UMR 1087, institut de recherche en santé de l'université de Nantes, 44007 Nantes cedex 1, France*

**KEYWORDS**
4D flow magnetic resonance imaging (MRI);
Phase-contrast magnetic resonance imaging;
Experimental studies;
Pulsatile flow model

**Abstract**
*Purpose:* The purpose of this study was to assess the precision of four-dimensional (4D) phase-contrast magnetic resonance imaging (PCMRI) to measure mean flow and peak velocity ($V_{max}$) in a pulsatile flow phantom and to test its sensitivity to spatial resolution and Venc.
*Material and methods:* The pulsatile flow phantom consisted of a straight tube connected to the systemic circulation of an experimental mock circulatory system. Four-dimensional-PCMR images were acquired using different spatial resolutions (minimum pixel size: $1.5 \times 1.5 \times 1.5\,mm^3$) and velocity encoding sensitivities (up to three times $V_{max}$). Mean flow and $V_{max}$ calculated from 4D-PCMRI were compared respectively to the reference phantom flow parameters and to $V_{max}$ obtained from two-dimensional (2D)-PCMRI.
*Results:* 4D-PCI measured mean flow with a precision of −0.04% to + 5.46%, but slightly underestimated $V_{max}$ when compared to 2D-PCMRI (differences ranging from −1.71% to −3.85%). 4D PCMRI mean flow measurement was influenced by spatial resolution ($P < 0.001$) with better

* Corresponding author.
*E-mail address:* art.dav44@gmail.com (A. David).

https://doi.org/10.1016/j.diii.2018.08.012

results obtained with smaller voxel size. There was no effect of Venc on mean flow measurement. Regarding $V_{max}$, neither spatial resolution nor Venc did influence the precision of the measurement.

*Conclusion:* Using an experimental pulsatile flow model 4D-PCMRI is accurate to measure mean flow and $V_{max}$ with better results obtained with higher spatial resolution. We also show that Venc up to 3 times higher than $V_{max}$ may be used with no effect on these measurements.



Four-dimensional (4D) phase contrast imaging (PCI) using magnetic resonance imaging (MRI) has been recently developed to allow a better understanding of blood flow through the heart and large vessels [1—3]. With 4D-PCI, velocity is encoded in all three spatial directions (i.e., three spatial dimensions) along the cardiac cycle (one temporal direction), resulting in a 4D model. Unlike two-dimensional (2D)-PCI or Doppler echocardiography, 4D-PCI can provide information on the spatial and temporal evolution of 3D blood flow within the boundaries of the volume covered [4]. In the past two decades, 4D-PCI acquisitions have been reported in a wide spectrum of anatomic locations such as heart [5], especially for congenital heart diseases [6], thoracic aorta [7], visceral vessels [8], or intracranial arteries [9]. Current disadvantages of 4D-PCI include limited spatial and temporal resolution for flow analysis adjacent to vessel walls [10] and long scan times ranging between 5 and 20 minutes depending on anatomic coverage, heart rate, and spatio-temporal resolution [4]. Several studies have compared 4D-PCI to current gold standard methods for in-vivo validation, such as Doppler examination or 2D-PCI, showing good correlation and reproducibility in various anatomic territories [11—17].

In clinical practice, incoherent measurements of flow and velocity in the heart and its great vessels raise concerns regarding the accuracy of the technique. Controlled pulsatile or steady flow phantom experiments can be used to assess accuracy for flow and velocity [18]. Hitherto, few studies have compared 4D-PCI to reference methods for in vitro measurement of flow parameters [19—24].

The purpose of this study was to assess the precision of 4D-PCI to measure mean flow and peak velocity ($V_{max}$) in a pulsatile flow phantom and to test its sensitivity to spatial resolution and Venc.

## Materials and methods

This work was a phantom study without any experimentation on humans. Therefore, Institutional review board approval and informed consent were not required.

### Flow phantom

To evaluate the quantitative accuracy of the 4D-PCI, in vitro velocity measurements were acquired on a pulsatile flow phantom previously designed in our center. The phantom consisted of a stiff straight tube with an inner diameter of 20 mm, surrounded by a box filled with agarose gel to minimize susceptibility artifacts and to mimic static tissues for background correction. The tube was filled with water and connected to polyvinyl chloride tubing leading out of the magnet room and was derived from the systemic circulation of an experimental mock circulatory system (Syncardia Systems, Inc.) [25]. This system simulated the systemic and pulmonary circulation and consisted of pulsatile left and right cardiac pumps (CardioWest™) connected with four tanks. Each artificial ventricle CardioWest™ consisted of a segmented cavity with two chambers, one with air content and the other with water content, separated by a polyurethane membrane. The four tanks corresponded to the aorta, the pulmonary artery and the two atria and contained different volumes of water. A flowmeter, placed between the tanks simulating the systemic circulation and the right atrium, provided the flow rate as a reference. The ventricles were powered by compressed air delivered from an external pneumatic controller, mobilizing the membrane and emptying the ejection chamber. Insufflation pressures in the ventricles, pulse rate and pressure levels in the tanks were calibrated to drive a pulsatile flow through the phantom at a rate of 100 beats per minute (bpm) with a mean flow of 4.8 L/min (Fig. 1).

### MRI acquisitions

Image acquisition of the flow phantom was performed on a clinical 1.5 T MRI unit (AERA®, Siemens Healthineers), using an 18-channel body matrix coil. A simulated electrocardiographic signal with a RR interval of 600 ms, corresponding to a pulse rate of 100 bpm, was used for gating.

For the 4D flow imaging, several 4D-PCI sequences with a 3D volume covering the flow phantom were acquired with different spatial resolutions and Venc to assess the accuracy of the sequence (Table 1). For 2D-PCI, images perpendicular to the straight tube were acquired with 60 frames per cycle, a field of view of 340 mm, a matrix of 192, a slab thickness of 6 mm, and the same Venc as for 4D-PCI acquisitions.

Mean flow (in mL/min), vessel area (in $mm^2$) and $V_{max}$ (in cm/sec) were calculated using a prototype investigational software — 4D Flow (Siemens Healthineers) for 4D flow acquisitions and using Argus® software (Siemens Healthineers) for 2D-PCI.

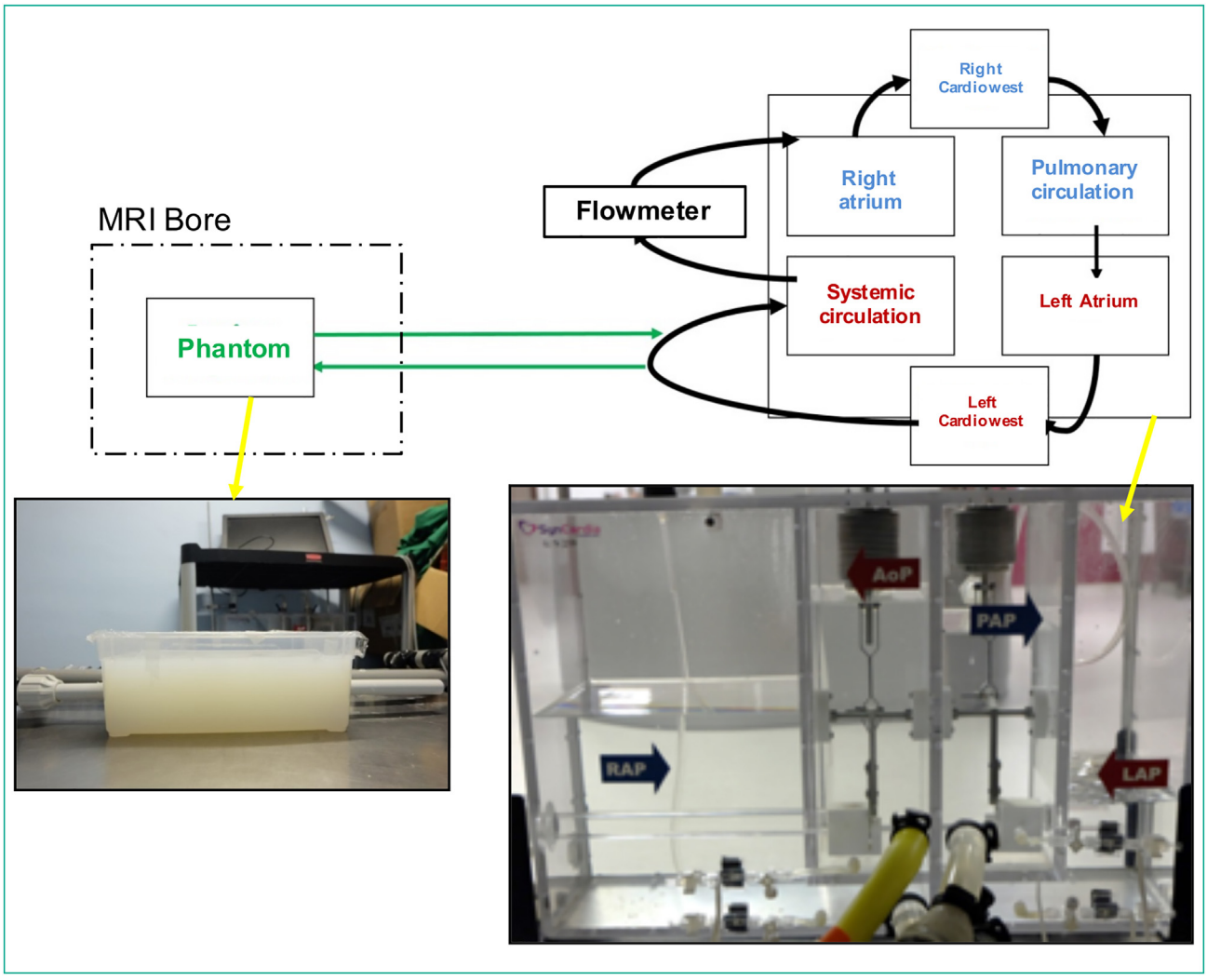


**Figure 1.** Schematic diagram of the experimental pulsatile flow model.

## Statistical analysis

The data were tabulated using an Excel 2013 spreadsheet (Microsoft) and statistical analysis were performed using XLSTAT and R. Quantitative variables were expressed as means ± standard deviation (SD) and ranges. Mean flow and vessel area calculated from 4D-PCI acquisitions were compared with the reference flow parameters (RFP) by a Wilcoxon test. Kruskal—Wallis and Wilcoxon tests were conducted to examine the differences between the results of 4D-PCI performed using different spatial resolutions and different Venc. In Wilcoxon tests, we compared peak velocities between 2D PC and 4D-PCI. Pearson's $r$ was used to describe the correlation between 2D-PCI and 4D-PCI for peak velocity measurement. Bland-Altman plots were generated comparing to 2D PCI and 4D-PCI for peak velocity measurement and the bias and limits of agreement were calculated. Significance was set at $P < 0.05$ (two-sided).

# Results

## Analysis of 4D-PCI mean flow and vessel area—comparison with experimental values

The results of the comparison of 4D-PCI derived mean flow and vessel area with RFP and the effects of spatial resolution and Venc are reported in Tables 2 and 3. 4D-PCI measured mean flow with a precision of −0.04% to + 5.46%, Regarding spatial resolution, significant differences were found in mean flow and vessel area ($P < 0.001$) between subgroups with identical Venc but different spatial resolutions. Better accuracy was obtained when smaller voxel sizes were used ($1.9 \times 1.9 \times 1.9$ and $1.5 \times 1.5 \times 1.5\,mm^3$) with no significant difference between these two highly resolved subgroups. Regarding Venc, Kruskal—Wallis tests showed no significant difference in mean flow and vessel area in subgroups with identical spatial resolution but different Venc (Fig. 2).

**Table 1** Four-dimensional phase contrast magnetic resonance imaging acquisition parameters.

| | Subgroup 1 | Subgroup 2 | Subgroup 3 | Subgroup 4 | Subgroup 5 |
|---|---|---|---|---|---|
| Mean flow = 4 L/min | | | | | |
| Venc (cm/sec) | 34 | 50 | 100 | 34 | 34 |
| Field of view (mm) | 360 | 360 | 360 | 360 | 320 |
| Matrix | 128 | 128 | 128 | 192 | 208 |
| Voxel size ($mm^3$) | $2.8 \times 2.8 \times 2.2$ | $2.8 \times 2.8 \times 2.2$ | $2.8 \times 2.8 \times 2.2$ | $1.9 \times 1.9 \times 1.9$ | $1.5 \times 1.5 \times 1.5$ |
| Repetition time (ms) | 50.48 | 48.50 | 41.92 | 52.00 | 53.12 |
| Echo time (ms) | 4.07 | 3.63 | 3.00 | 4.08 | 4.12 |
| Frames per cycle | 30 | 30 | 30 | 30 | 30 |
| Mean Flow = 5.6 L/min | | | | | |
| Venc (cm/sec) | 50 | 75 | 150 | 50 | 50 |
| Field of view (mm) | 360 | 360 | 360 | 360 | 320 |
| Matrix | 128 | 128 | 128 | 192 | 208 |
| Voxel size ($mm^3$) | $2.8 \times 2.8 \times 2.2$ | $2.8 \times 2.8 \times 2.2$ | $2.8 \times 2.8 \times 2.2$ | $1.9 \times 1.9 \times 1.9$ | $1.5 \times 1.5 \times 1.5$ |
| Repetition time (ms) | 48.50 | 43.76 | 39.92 | 48.48 | 49.52 |
| Echo time (ms) | 3.63 | 3.23 | 2.75 | 3.64 | 3.67 |
| Frames per cycle | 30 | 30 | 30 | 30 | 30 |

**Table 2** Mean flow measured in four-dimensional phase contrast magnetic resonance imaging (4D-PCI) and compared to reference experimental value.

| | *n* | Spatial resolution ($mm^3$) | Venc (cm/sec) | Mean Flow (ml/min) | Difference |
|---|---|---|---|---|---|
| Reference value | | | | 4800 | – |
| 4D-PCI Total | 100 | | | 4942.65 ± 873.91 [3652.8–6339.6] | +142.65 (+2.97%) |
| 4D-PCI Subgroup 1 | 20 | $2.8 \times 2.8 \times 2.2$ | 42 | 5048.82 ± 903.80 [3798–6224.4] | +248.82 (+5.18%) |
| 4D-PCI Subgroup 2 | 20 | $2.8 \times 2.8 \times 2.2$ | 62.5 | 5010.57 ± 882.56 [3903–6189] | +210.57 (+4.39%) |
| 4D-PCI Subgroup 3 | 20 | $2.8 \times 2.8 \times 2.2$ | 125 | 5062.11 ± 922.57 [3797.4–6339.6] | +262.11 (+5.46%) |
| 4D-PCI Subgroup 4 | 20 | $1.9 \times 1.9 \times 1.9$ | 42 | 4798.31 ± 798.32 [3809.4–5848.2] | −1.69 (−0.04%) |
| 4D-PCI Subgroup 5 | 20 | $1.5 \times 1.5 \times 1.5$ | 42 | 4793.43 ± 904.44 [3652.8–5808.6] | −6.57 (−0.14%) |

Results are expressed as mean ± standard deviation (SD). Numbers in bracket are ranges.

**Table 3** Vessel area measured in four-dimensional phase contrast magnetic resonance imaging (4D-PCI) and compared to reference experimental value.

| | *n* | Spatial resolution ($mm^3$) | Venc (cm/sec) | Vessel area ($mm^2$) | Difference |
|---|---|---|---|---|---|
| Reference value | | | | 314.16 | – |
| 4D-PCI Total | 100 | | | 370.5 ± 26.26 [303.8–424.6] | +56.34 (+17.93%) |
| 4D-PCI Subgroup 1 | 20 | $2.8 \times 2.8 \times 2.2$ | 42 | 384.53 ± 26.33 [325.5–424.6] | +70.37 (+22.40%) |
| 4D-PCI Subgroup 2 | 20 | $2.8 \times 2.8 \times 2.2$ | 62.5 | 382.92 ± 22.73 [337.4–424.5] | +68.76 (+21.89%) |
| 4D-PCI Subgroup 3 | 20 | $2.8 \times 2.8 \times 2.2$ | 125 | 378.66 ± 23.27 [331.8–422.5] | +64.50 (+20.53%) |
| 4D-PCI Subgroup 4 | 20 | $1.9 \times 1.9 \times 1.9$ | 42 | 353.62 ± 16.53 [309.7–378.2] | +39.46 (+12.56%) |
| 4D-PCI Subgroup 5 | 20 | $1.5 \times 1.5 \times 1.5$ | 42 | 370.5 ± 26.26 [303.8–424.6] | +56.34 (+17.93%) |

Results are expressed as mean ± standard deviation (SD). Numbers in bracket are ranges.

## Analysis of 4D-PCI $V_{max}$ —comparison with 2D-PCI

The results of the comparison of 4D-PCI derived Vmax with 2D-PCI and the effects of spatial resolution and Venc are reported in Table 4. 4D-PCI slightly underestimated $V_{max}$ when compared to 2D-PCI (differences ranging from −1.71% to −3.85%; $P < 0.001$). Correlation was excellent between the two modalities ($r = 0.962$; 95%CI: 0.944–0.974; $P < 0.001$). Bland–Altman tests showed a mean of differences (bias) of −2.83% of the overall mean value for $V_{max}$ between 2D PC and 4D-PCI, with limits of agreement

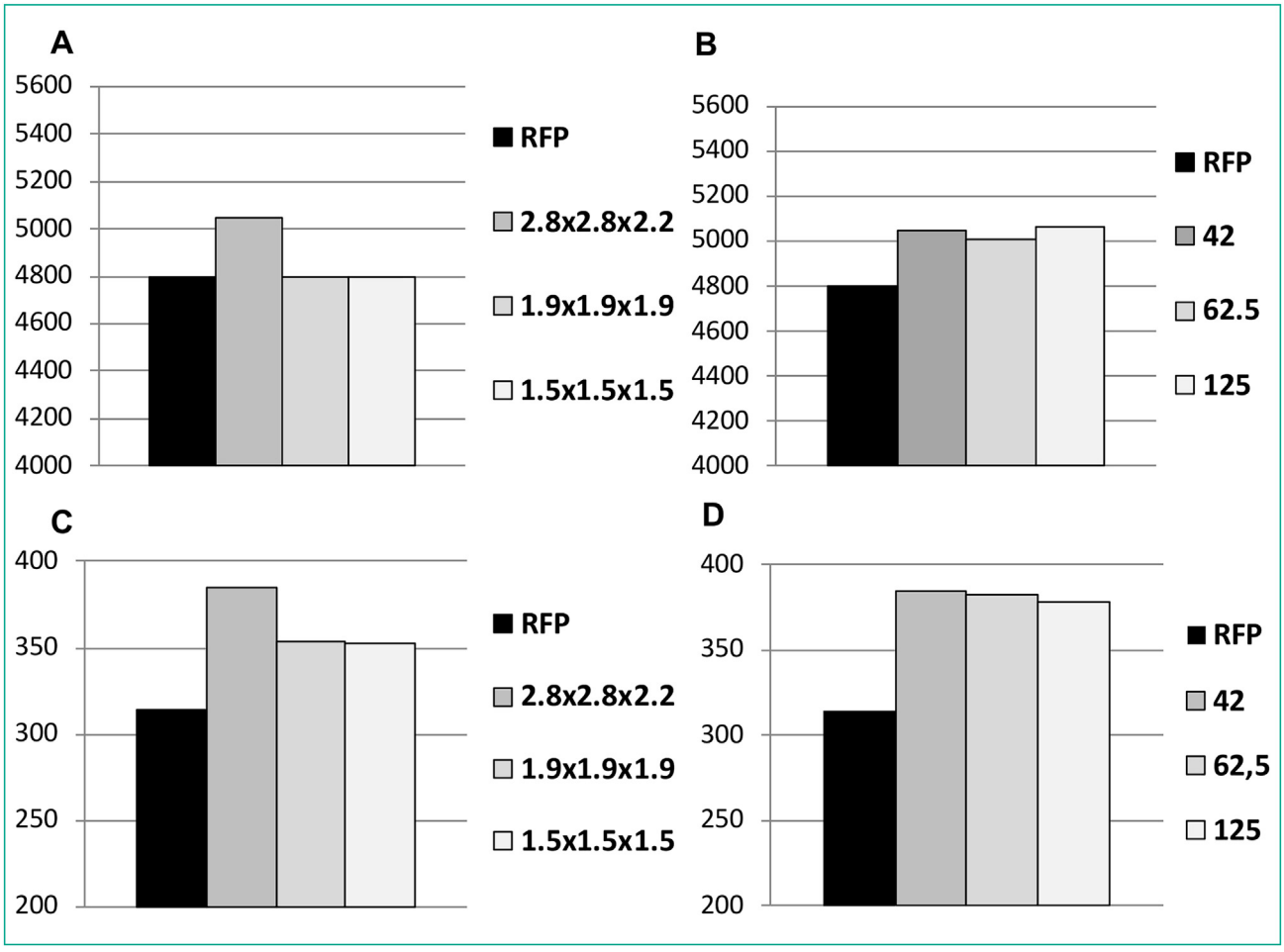


**Figure 2.** Column bars show flow and vessel area measured with 4D-PCI and compared to reference experimental values. A. Comparison of subgroups with different spatial resolutions but identical Venc for mean flow measurements. B. Comparison of subgroups with different Venc but identical spatial resolutions for mean flow measurements. C. Comparison of subgroups with different spatial resolutions but identical Venc for vessel area measurements. D. Comparison of subgroups with different Venc but identical spatial resolutions for vessel area measurements.

**Table 4** Peak velocity measured in four-dimensional phase contrast magnetic resonance imaging (4D-PCI) and compared to reference two-dimensional phase contrast magnetic resonance imaging (2D-PCI) values.

| | *n* | 2D-PCI Peak velocity (cm/sec) | Spatial resolution ($mm^3$) | Venc (cm/sec) | 4D-PCI Peak velocity (cm/sec) | Difference |
|---|---|---|---|---|---|---|
| Total | 100 | 35.80 ± 5.59 [26.88—47.78] | | | 34.78 ± 4.98 [27.69—41.03] | −1.01 (−2.83%) |
| Subgroup 1 | 20 | 35.49 ± 4.88 [29.3—41] | 2.8 × 2.8 × 2.2 | 42 | 34.88 ± 5.05 [28.02—40.19] | −0.61 (−1.71%) |
| Subgroup 2 | 20 | 35.67 ± 5.98 [26—43.07] | 2.8 × 2.8 × 2.2 | 62.5 | 34.37 ± 5.03 [28.56—40.23] | −1.31 (−3.66%) |
| Subgroup 3 | 20 | 35.07 ± 5.14 [27.67—47.78] | 2.8 × 2.8 × 2.2 | 125 | 35.07 ± 5.14 [28.84—41.03] | −0.84 (−2.34%) |
| Subgroup 4 | 20 | 34.66 ± 5.06 [29.17—43.08] | 1.9 × 1.9 × 1.9 | 42 | 34.66 ± 5.06 [27.92—39.93] | −1.39 (−3.85%) |
| Subgroup 5 | 20 | 35.88 ± 5.1 [29.8—41.65] | 1.5 × 1.5 × 1.5 | 42 | 34.9 ± 5.1 [27.69—40.13] | −0.93 (−2.59%) |

Results are expressed as mean ± standard deviation (SD). Numbers in bracket are ranges.

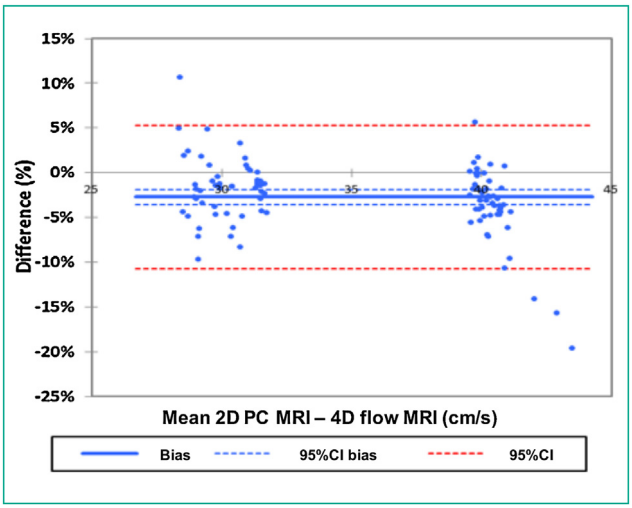


**Figure 3.** Diagram shows Bland—Altman plots of 4D-PCI compared with 2D-PCI for $V_{max}$ measurement.

between −10.71% and +5.29% (Fig. 3). There were no significant differences between groups with varied spatial resolution ($P = 0.74$), nor in groups with varied Venc ($P = 0.39$).

## Discussion

We developed an experimental methodology to evaluate the accuracy of 4D-PCI flow measurements in a 20-mm straight tube. We showed that 4D-PCI is accurate at measuring mean flow with better results obtained with higher spatial resolution and conversely no effect of Venc when varied up to 3 times $V_{max}$. A good agreement between 4D-PCI and 2D-PCI was found for the measurement of $V_{max}$.

Long time scans are needed to acquire 4D-PCI especially when using small pixel size. One objective of this work was therefore to evaluate the impact of increasing the spatial resolution on the accuracy of 4D-PCI measurements. Indeed, in our present in vitro study, we were able to demonstrate that an increase in the spatial resolution improved the measurement of vessel area and mean flow, which are directly related to the quality of the segmentation. With higher spatial resolution images, the accuracy of the segmentation minimizes partial volume effects near to the boundaries of the tube, providing better flow measurements. These results are consistent with those of Kweon et al. who reported a higher accuracy of mean flow measurements on a phantom when increasing 4D flow spatial resolutions [21]. One should note however that in our study, although results were better with 1.9 mm and with 1.5 mm isotropic spatial resolution than with $2.8 \times 2.8 \times 2.2$ mm resolution, 1.5 mm isotropic resolution did not provide significantly better results than 1.9-mm isotropic resolution. This result may be explained by the reduction of the signal-to-noise ratio caused by an important increase of spatial resolution, as suggested by Kweon et al. [21]. Although in theory, a higher resolution may give a better estimation of flow measurements, considering the signal-to-noise ratio reduction and the longer scan time, refining the voxel size below 1.9-mm isotropic might not be useful under the present conditions. This also supports the strategy of super-resolution at stage of post-processing so that SNR remains high.

To evaluate the valvular or arterial stenosis severity, one of the most important parameter is $V_{max}$ [26]. In the present study, no differences were found between low and high spatial resolution subgroups. This may be due to the fact that the peak intensity voxel is commonly located in the central region of the tube, and thereby less dependent of the quality of the segmentation. Some authors have reported that improving spatial resolution may lead to a better estimation of $V_{max}$ by 4D-PCI [21]. However, the spatial resolution of their reference standard, (computational fluid dynamics) was markedly higher than 2D-PCI. Our data suggests that current spatial resolution ($2.8 \times 2.8 \times 2.2$ in our study) may be sufficient to provide reliable results regarding this hemodynamic parameter.

A second objective of this study was to assess the impact of Venc on the measurement of hemodynamic parameters with 4D-PCI. We found that there was no significant difference for all the measured flow parameters when using Venc between a velocity equal to Vmax and a velocity three times greater. This low variation using low or high Venc may be useful in clinical practice, as only one Venc is allowed for the acquisition of the 4D-PCI sequence and as it is imperative that Venc is largely higher than Vmax to avoid saturation. This is particularly true when studying patients with arterial of valvular stenosis, which generates high velocities and velocity aliasing.

This study has some limitations, especially regarding the flow conditions in our experimental model. For example, the use of a non-MRI compatible pump to generate the flow made it necessary to lengthen the water circuit, thus impeding residual pulsatility within the measurement tube. Indeed, the ratio between peak and mean velocities was only 1.54. Additionally, analysis of axial velocity profiles across the tube showed that axial velocity remained positive throughout the cycle, without return to zero. The tube was rigid, limiting the analysis of vascular compliance. Our experimental model was filled with water, whose viscosity is about $10^{-6}\,m^2.s^{-1}$ (versus $4.10^{-6}\,m^2$ for blood). Finally, regarding $V_{max}$, one should note that our phantom allowed us to reach a peak of nearly 40 cm/s only, which is lower that peak velocities found in clinical practice for valvular and arterial diseases. We therefore chose low Venc, far from those used in clinical practice, so that they were higher than Vmax, but still close to it in order to maintain a sufficient signal-to-noise ratio. Future changes in our model, including smaller tubes (allowing higher velocities) and the use of blood-equivalent fluid, should be made in order to obtain more physiologic hemodynamic conditions. Moreover, one should note that these low velocities make our results only valid in turbulent free conditions, which are found in vivo in areas located away from stenosis and valves. Assessment of the accuracy of 4D-PCI in a turbulent environment will be the scope of future studies.

In conclusion, using an experimental pulsatile flow model we showed that 4D-PCI is accurate to measure mean flow and $V_{max}$ with better results obtained with higher spatial resolution. We also show that Venc up to 3 times higher than Vmax may be used with no effect on these measurements.

## Disclosure of interest

The authors declare that they have no competing interest.

## References


[1] Firmin DN, Gatehouse PD, Konrad JP, Yang GZ, Kilner PJ, Longmore DB. Rapid 7-dimensional imaging of pulsatile flow. Comput Cardiol IEEE Comput Soc Lond 1993;14:353—6.

[2] Wigström L, Sjoqvist L, Wranne B. Temporally resolved 4D phase-contrast imaging. Magn Reson Med 1996;36:800—3.

[3] Markl M, Chan FP, Alley MT, Wedding KL, Draney MT, Elkins CJ, et al. Time-resolved three-dimensional phase-contrast MRI. J Magn Reson Imaging 2003;17:499—506.

[4] Stankovic Z, Markl M. 4D flow imaging with MRI. Cardiovasc Diagn Ther 2014;4:173—92.

[5] Bolger AF, Heiberg E, Karlsson M, Wigström L, Engvall J, Sigfridsson A, et al. Transit of blood flow through the human left ventricle mapped by cardiovascular magnetic resonance. J Cardiovasc Magn Reson 2007;9:741—7.

[6] Markl M, Geiger J, Kilner PJ, Föll D, Stiller B, Beyersdorf F, et al. Time-resolved three-dimensional magnetic resonance velocity mapping of cardiovascular flow paths in volunteers and patients with Fontan circulation. Eur J Cardiothorac Surg 2011;39:206—12.

[7] Bürk J, Blanke P, Stankovic Z, Barker A, Russe M, Geiger J, et al. Evaluation of 4D blood flow patterns and wall shear stress in the normal and dilated thoracic aorta using flow-sensitive 4D CMR. J Cardiovasc Magn Reson 2012;14:84.

[8] Bächler, Pinochet N, Sotelo J, Crelier G, Irarrazaval P, Tejos C, et al. Assessment of normal flow patterns in the pulmonary circulation by using 4D magnetic resonance velocity mapping. Magn Reson Imaging 2013;31:178—88.

[9] Bammer R, Hope TA, Aksoy M, Alley MT. Time-resolved 4D quantitative flow MRI of the major intracranial vessels: initial experience and comparative evaluation at 1.5 T and 3.0 T in combination with parallel imaging. Magn Reson Med 2007;57:127—40.

[10] Boussel L, Rayz V, Martin A, Acevedo-Bolton G, Lawton MT, Higashida R, et al. Phase-contrast magnetic resonance imaging measurements in intracranial aneurysms in vivo of flow patterns, velocity fields, and wall shear stress: comparison with computational fluid dynamics. Magn Reson Med 2009;61:409—17.

[11] Meckel S, Stalder AF, Santini F, Radü EW, Rüfenacht DA, Markl M, et al. In vivo visualization and analysis of 3-D hemodynamics in cerebral aneurysms with flow-sensitized 4-D MR imaging at 3 T. Neuroradiology 2008;50:473—84.

[12] Frydrychowicz A, Markl M, Hirtler D, Harloff A, Schlensak C, Geiger J, et al. Aortic hemodynamics in patients with and without repair of aortic coarctation: in vivo analysis by 4D flow-sensitive magnetic resonance imaging. Invest Radiol 2011;46:317—25.

[13] Stankovic Z, Csatari Z, Deibert P, Euringer W, Blanke P, Kreisel W, et al. Normal and altered three-dimensional portal venous hemodynamics in patients with liver cirrhosis. Radiology 2012;262:682—773.

[14] Wentland AL, Grist TM, Wieben O. Repeatability and internal consistency of abdominal 2D and 4D phase contrast MR flow measurements. Acad Radiol 2013;20:699—704.

[15] Meckel S, Leitner L, Bonati LH, Santini F, Schubert T, Stalder AF, et al. Intracranial artery velocity measurement using 4D PC MRI at 3 T: comparison with transcranial ultrasound techniques and 2D PC MRI. Neuroradiology 2013;55:389—98.

[16] Markl M, Wallis W, Harloff A. Reproducibility of flow and wall shear stress analysis using flow-sensitive four-dimensional MRI. J Magn Reson Imaging 2011;33:988—94.

[17] Nordmeyer S, Riesenkampff E, Crelier G, Khasheei A, Schnackenburg B, Berger F, et al. Flow-sensitive four-dimensional cine magnetic resonance imaging for offline blood flow quantification in multiple vessels: a validation study. J Magn Reson Imaging 2010;32:677—83.

[18] Dyverfeldt P, Bissel M, Barker AJ, Bolger AF, Carlhäll CJ, Ebbers T, et al. 4D flow cardiovascular magnetic resonance consensus statement. J Cardiovasc Magn Reson 2015;17:72.

[19] Gu T, Korosec FR, Block WF, Fain SB, Turk Q, Lum D, et al. PC VIPR: a high-speed 3D phase-contrast method for flow quantification and high-resolution angiography. AJNR Am J Neuroradiol 2005;26:743—9.

[20] Ghosn MG, Jackson M, Maragiannis D, Chin K, Autry K, Igo S, et al. An in vitro validation of cardiac magnetic resonance 4D flow measurements with bioprosthetic mitral valve flow volumes quantification. J Cardiovasc Magn Reson 2014;16:67.

[21] Kweon J, Yang DH, Kim CB, Kim N, Paek M, Stalder AF, et al. Four-dimensional flow MRI for evaluation of post-stenotic turbulent flow in a phantom: comparison with flowmeter and computational fluid dynamics. Eur Radiol 2016;26:3588—97.

[22] Zhao SZ, Papathanasopoulou P, Long Q, Marshall I, Xu XY. Comparative study of magnetic resonance imaging and image-based computational fluid dynamics for quantification of pulsatile flow in a carotid bifurcation phantom. Ann Biomed Eng 2003;31:962—71.

[23] Hollnagel DI, Summers PE, Poulikakos D, Kollias SS. Comparative velocity investigations in cerebral arteries and aneurysms: 3D phase-contrast MR angiography, laser Doppler velocimetry and computational fluid dynamics. NMR Biomed 2009;22:795—808.

[24] Hollnagel DI, Summers PE, Kollias SS, Poulikakos D. Laser Doppler velocimetry (LDV) and 3D phase-contrast magnetic resonance angiography (PC-MRA) velocity measurement: validation in an anatomically accurate cerebral artery aneurysm model with steady flow. J Magn Reson Imaging 2007;26:1493—505.

[25] Senage T, Fevrier D, Michel M, Pichot E, Duveau D, Tsui S, et al. A mock circulatory system to assess the performance of continuous-flow left ventricular assist devices (LVADs): does axial flow unload better than centrifugal LVAD? ASAIO J 2014;60:140—7.

[26] Gach P, Dabadie A, Sorensen C, Quarello E, Bonello B, Pico H, et al. Multimodality imaging of aortic coarctation: from the fetus to the adolescent. Diagn Interv Imaging 2016;97:581—90.